



Short Communication

Electromagnetic scattering by spheroidal volumes of discrete random medium

Michael I. Mishchenko^{a,*}, Janna M. Dlugach^b^aNASA Goddard Institute for Space Studies, 2880 Broadway, New York, NY 10025, USA^bMain Astronomical Observatory of the National Academy of Sciences of Ukraine, 27 Zabolotny Str., 03680, Kyiv, Ukraine

ARTICLE INFO

Article history:

Received 18 May 2017

Revised 18 June 2017

Accepted 20 June 2017

Available online 21 June 2017

Keywords:

Electromagnetic scattering

Multi-particle groups

Discrete random medium

Radiative transfer theory

Coherent backscattering

ABSTRACT

We use the superposition T -matrix method to compare the far-field scattering matrices generated by spheroidal and spherical volumes of discrete random medium having the same volume and populated by identical spherical particles. Our results fully confirm the robustness of the previously identified coherent and diffuse scattering regimes and associated optical phenomena exhibited by spherical particulate volumes and support their explanation in terms of the interference phenomenon coupled with the order-of-scattering expansion of the far-field Foldy equations. We also show that increasing nonsphericity of particulate volumes causes discernible (albeit less pronounced) optical effects in forward and backscattering directions and explain them in terms of the same interference/multiple-scattering phenomenon.

Published by Elsevier Ltd.

1. Introduction

The use of direct, numerically exact computer solvers of the macroscopic Maxwell equations to study electromagnetic scattering by volumes of discrete random medium (DRM) has been a hot topic over the past decade (see, e.g., Refs. [1–6] and the comprehensive reference list in the recent review [7]). In particular, the effects of domain size [8], particle size [9], particle refractive index [1,9] (including the imaginary part [10]), and particle packing density [11,12] have been studied in substantial detail. In many publications the statistical randomness of particle positions has been modeled by first running a random-number generator to assign coordinates of N particles quasi-randomly filling a spherical volume of DRM and then averaging over the uniform orientation distribution of the resulting multi-particle configuration (e.g., [1,7] and references therein). Several numerical tests have shown that this approach yields highly repeatable far-field scattering patterns irrespectively of the initial quasi-random set of particle positions within the volume, in a stark contrast to the patterns caused by fully ordered multi-particle configurations in random orientation [13]. Furthermore, the use of the analytical orientation-averaging procedure afforded by the superposition T -matrix method [14,15] completely eliminates residual statistical “noise” in the angular scattering patterns caused by brute-force numerical ensemble averaging (see, e.g., Refs. [16,17]). The result-

ing numerical data have been used to study the suppression of the speckle pattern upon ensemble averaging as well as to identify definitively the coherent forward-scattering, diffuse radiative-transfer, and coherent backscattering regimes and their strong dependence on particle characteristics [1,7,18].

The majority of the results thus obtained have relied on the superposition T -matrix method and (with the exception of a cube [16] and a cylindrical slab [19] in fixed orientation) on the simplest model of a DRM in the form of a (statistically) spherical particulate volume in random orientation (e.g., [1,7,18]). Importantly, however, this technique is not restricted to spherical volumes of DRM and can be applied effectively to, e.g., spheroidal volumes. This makes it possible to analyze whether the main conclusions of the previous studies reviewed in Ref. [7] remain intact in the case of randomly oriented nonspherical volumes of DRM and whether nonsphericity leads to new discernable effects.

The main objective of this Short Communication is to perform such an analysis. In the following section we briefly introduce the requisite terminology and notation and describe the modeling methodology used in our analysis. The final section contains a discussion and summary of our findings.

2. Modeling methodology

Our analysis parallels that in Refs. [1,7,18] and is based on the comparison of far-field scattering matrices generated by spheroidal as well as spherical volumes of DRM having the same volume V and populated by identical spherical particles. In all computations,

* Corresponding author.

E-mail address: michael.i.mishchenko@nasa.gov (M.I. Mishchenko).

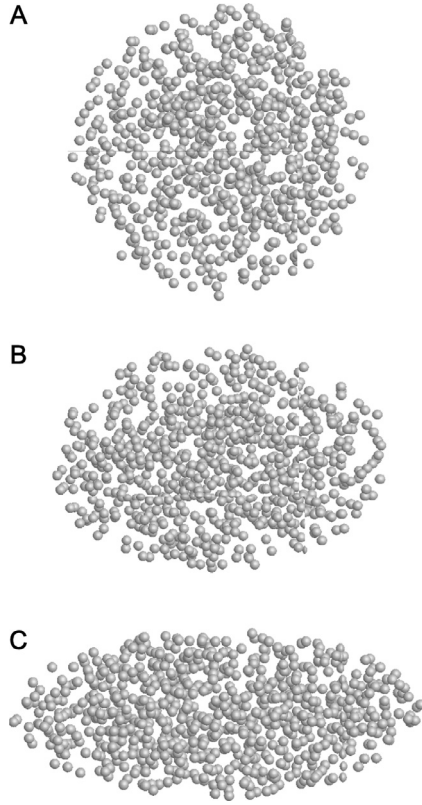


Fig. 1. V-equivalent spherical (panel A) and oblate spheroidal (panels B and C) volumes of discrete random medium populated quasi-randomly by $N=800$ identical spherical particles. The aspect ratio E is 1.5 in panel B and 2.5 in panel C. The volumes are viewed perpendicularly to their short axes.

the particle radius r is fixed at a value implying the particle size parameter $kr=2$, where k is the wave number in the host medium, while the refractive index of the particles is fixed at $m=1.31$. These specific values are expected to help identify the presence of the polarization opposition effect [8] observed both in the laboratory [20,21] and in telescopic observations for a class of high-albedo solar system bodies [22,23]. The radius of the spherical volumes R is fixed at a value implying the volume size parameter $kR=60$. The shape of a prolate or oblate spheroid is defined by its aspect ratio E , i.e., the ratio of the longest to the shortest spheroidal axes, while the lengths of the axes are defined by the requirement that the spheroid have the same volume V .

The initial particle coordinates inside a spherical or spheroidal volume are assigned by running a random-number generator developed by D. W. Mackowski (personal communication; see Ref. [24]) and making sure that the particles do not overlap (see examples of multi-sphere configurations representing spherical and spheroidal volumes of DRM in Fig. 1). This is followed by the summation of the light-scattering results obtained by averaging over the equiprobable orientation distribution of the particulate volume and of its mirror counterpart. It is well known [25,26] that the outcome of this procedure is the symmetric block-diagonal normalized scattering matrix given by

$$\tilde{\mathbf{F}}(\Theta) = \begin{bmatrix} \tilde{F}_{11}(\Theta) & \tilde{F}_{12}(\Theta) & 0 & 0 \\ \tilde{F}_{12}(\Theta) & \tilde{F}_{22}(\Theta) & 0 & 0 \\ 0 & 0 & \tilde{F}_{33}(\Theta) & \tilde{F}_{34}(\Theta) \\ 0 & 0 & -\tilde{F}_{34}(\Theta) & \tilde{F}_{44}(\Theta) \end{bmatrix} \quad (1)$$

with

$$\tilde{F}_{12}(0) = \tilde{F}_{34}(0) = \tilde{F}_{12}(\pi) = \tilde{F}_{34}(\pi) = 0, \quad (2)$$

where $\Theta \in [0, \pi]$ is the scattering angle (i.e., the angle between the incidence and scattering directions) and the (1,1) element (i.e., the phase function) satisfies the standard normalization condition

$$\frac{1}{2} \int_0^\pi d\Theta \tilde{F}_{11}(\Theta) \sin \Theta = 1. \quad (3)$$

Note that the scattering matrix of Eq. (1) is that expected as the asymptotic result of ensemble averaging over an infinite number of quasi-random realizations of a particulate volume. We have demonstrated previously that averaging over all orientations of a single quasi-random realization already yields results representative of those obtained by ensemble averaging. Yet the off-block-diagonal elements, while being much smaller than the block-diagonal ones in the absolute-value sense, do not vanish completely. Therefore, the purpose of averaging over the equiprobable orientation distribution of the particulate volume and of its mirror counterpart is to yield the scattering matrix (1) with the off-block-diagonal elements precisely equal to zero. We have verified that doing that with the superposition T -matrix method is in fact numerically equivalent to an artificial symmetrization wherein the off-block-diagonal elements computed for a randomly oriented quasi-random multiparticle group are zeroed out without adding the scattering matrix for the mirror counterpart of the group.

All numerical computations have been performed on the distributed-memory computer cluster of the Main Astronomical Observatory of the Ukrainian National Academy of Sciences using the parallelized version of the superposition T -matrix method described in Ref. [15].

3. Discussion and conclusions

Fig. 2 displays all six independent elements of the normalized scattering matrix for a spherical volume of DRM with $N=800$ and those of the V- and N-equivalent oblate spheroidal volume with $E=2.5$. It is remarkable that despite a large difference in the shapes of the two volumes (Fig. 1), the corresponding scattering matrices are very similar. Both phase functions reveal the following common traits:

- a strong coherent forward-scattering effect in the form of almost identical sharp “diffraction” peaks centered at $\Theta=0$;
- a very smooth and featureless diffuse background at scattering angles extending from 20° to 170° ; and
- a coherent backscattering peak centered at $\Theta=180^\circ$.

All three traits are discussed in Refs. [1,7] and explained in the framework of the order-of-scattering expansion of the far-field Foldy equations. Furthermore, the degree of linear polarization for unpolarized incident light (i.e., the ratio $-\tilde{F}_{12}(\Theta)/\tilde{F}_{11}(\Theta)$) exhibits the coherent polarization opposition effect in the form of a narrow minimum at backscattering angles [27]. The qualitative explanation of this phenomenon is given in Refs. [8,28].

Consistent with their interference nature, all manifestations of coherent backscattering intensify with increasing N . This is illustrated in Fig. 3 displaying the ratio $-\tilde{F}_{12}(\Theta)/\tilde{F}_{11}(\Theta)$ and the quantity $[\tilde{F}_{11}(\Theta) - \tilde{F}_{22}(\Theta)]/2$. The latter describes the angular distribution of the cross-polarized scattered intensity in the case of linearly polarized incident light. It is seen indeed that the depth of the backscattering polarization minimum doubles as N increases from 400 to 800, while the height of the backscattering peak in $[\tilde{F}_{11}(\Theta) - \tilde{F}_{22}(\Theta)]/2$ grows by a factor of 1.8.

The results of extensive computations for oblate and prolate spheroidal volumes of DRM with $400 \leq N \leq 800$ and $1 \leq E \leq 2$ are quite analogous to those in Figs. 2 and 3 and therefore are not shown.

Despite the somewhat surprising similarity of the $E=1$ and $E=2.5$ curves in Fig. 2, we can clearly identify two additional ef-

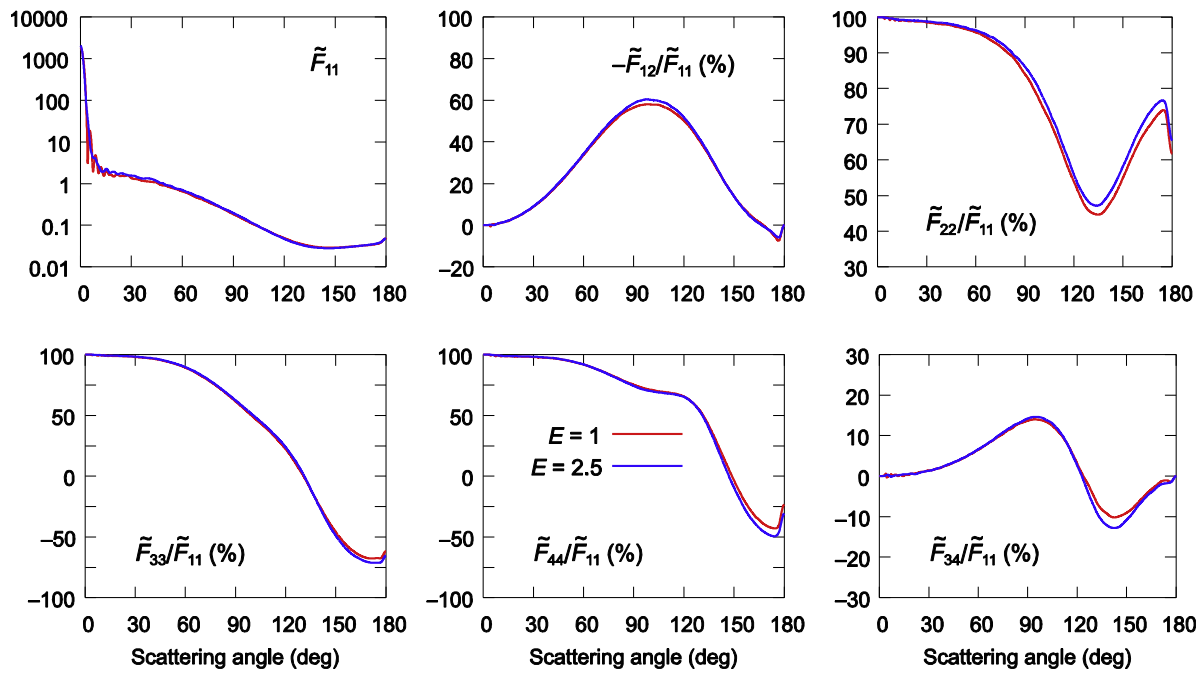


Fig. 2. Elements of the normalized scattering matrix $\tilde{F}(\Theta)$ for spherical and oblate spheroidal volumes with $E = 1$ and 2.5 , respectively, each populated by $N = 800$ identical spherical particles.

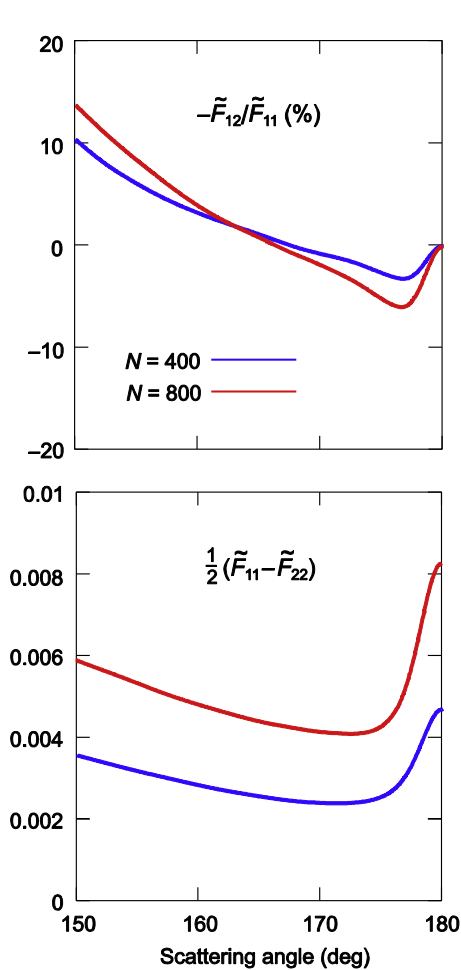


Fig. 3. Coherent backscattering features exhibited by oblate $E = 2.5$ spheroidal volumes populated by $N = 400$ and 800 identical spherical particles.

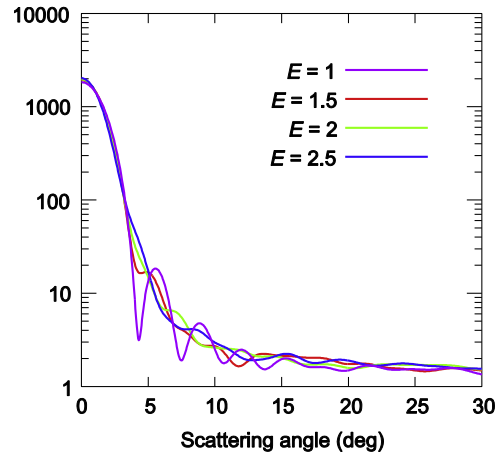


Fig. 4. Phase function $\tilde{F}_{11}(\Theta)$ for spherical and oblate spheroidal volumes with $E = 1, 1.5, 2,$ and 2.5 , each filled with $N = 800$ identical spherical particles.

facts caused by nonsphericity of a particulate volume. First, Fig. 4 shows that the pronounced interference pattern exhibited by the spherical volume at scattering angles ranging from 5° to 20° becomes attenuated with increasing E and essentially vanishes for $E = 2.5$. This smoothing effect can be explained by the continuous change of the geometrical projection of a spheroidal volume on a plane normal to the incidence direction during the process of averaging over orientations. The range of geometrical projections grows with increasing E , which results in progressively smooth “diffraction” patterns outside the main peak centered at $\Theta = 0$. One can of course expect that averaging the forward-scattering interference pattern of a spherical particulate volume over R would have a similar smoothing effect.

Second, Fig. 5 demonstrates the effect of increasing asphericity of a particulate volume on the degree of linear polarization $-\tilde{F}_{12}(\Theta)/\tilde{F}_{11}(\Theta)$ as well as on the backscattering linear and circular

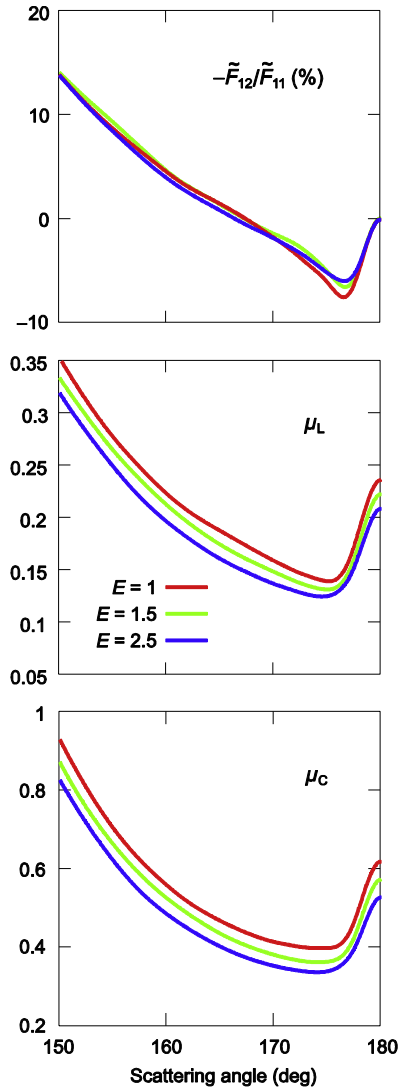


Fig. 5. Degree of linear polarization and linear and circular polarization ratios for spherical and oblate spheroidal volumes with $E = 1, 1.5,$ and $2.5,$ each populated by $N = 800$ identical spherical particles.

polarization ratios defined, respectively, by

$$\mu_L(\Theta) = \frac{\tilde{F}_{11}(\Theta) - \tilde{F}_{22}(\Theta)}{\tilde{F}_{11}(\Theta) + 2\tilde{F}_{12}(\Theta) + \tilde{F}_{22}(\Theta)} \quad (4)$$

and

$$\mu_C(\Theta) = \frac{\tilde{F}_{11}(\Theta) + \tilde{F}_{44}(\Theta)}{\tilde{F}_{11}(\Theta) - \tilde{F}_{44}(\Theta)}. \quad (5)$$

In the exact backscattering direction ($\Theta = 180^\circ$), both polarization ratios are equal to zero for a single spherical particle, which makes them sensitive indicators of the amount of multiple scattering in groups of particles and the resulting coherent backscattering. It is seen from Fig. 5 that both $\mu_L(\Theta)$ and $\mu_C(\Theta)$ decrease with increasing asphericity, which can easily be explained. Indeed, the average length of multi-particle sequences contributing to the scattered signal can be expected to decrease as the particulate volume becomes progressively flat as a consequence of its axis of rotational symmetry becoming significantly smaller than its lateral axes (Fig. 1). This results in less multiple scattering and thus in weaker μ_L and μ_C peaks centered at $\Theta = 180^\circ$ and caused by coherent backscattering. For the same reason, the minimum in the $-\tilde{F}_{12}(\Theta)/\tilde{F}_{11}(\Theta)$ curves caused by coherent backscattering (see the

upper panel of Fig. 5) becomes shallower with increasing asphericity of the particulate volume.

Thus we can conclude that the superposition T -matrix results for spheroidal particulate volumes fully confirm the robustness of the scattering regimes and optical phenomena exhibited by spherical volumes of DRM as well as supports their qualitative and quantitative explanations given in Ref. [7] (see also Refs. [29,30]). This conclusion may have practical implications, for example in the qualitative interpretation of opposition optical phenomena exhibited by the particulate icy bodies forming Saturn's rings [27,31]. Furthermore, increasing nonsphericity of particulate volumes causes discernable (albeit less pronounced) optical effects that can also be explained in terms of the interference phenomenon coupled with the order-of-scattering expansion of the far-field Foldy equations.

Acknowledgments

We thank Nadia Zakharova for help with graphics and three anonymous reviewers for their constructive comments. This material is based upon work supported by the NASA Remote Sensing Theory Program managed by Lucia Tsaoussi. JMD acknowledges support from the National Academy of Sciences of Ukraine under the Main Astronomical Observatory GRAPE/GPU/GRID Computing Cluster Project.

References

- [1] Mishchenko MI, Liu L, Mackowski DW, Cairns B, Videen G. Multiple scattering by random particulate media: exact 3D results. *Opt Express* 2007;15:2822–36.
- [2] Tseng SH, Huang B. Comparing Monte Carlo simulation and pseudospectral time-domain numerical solutions of Maxwell's equations of light scattering by a macroscopic random medium. *Appl Phys Lett* 2007;91:051114.
- [3] Sukhov A, Haefner D, Dogariu A. Coupled dipole method for modeling optical properties of large-scale random media. *Phys Rev E* 2008;77:066709.
- [4] Penttilä A. Quasi-specular reflection from particulate media. *J Quant Spectrosc Radiat Transf* 2013;131:130–7.
- [5] Mackowski D. Van de Hulst Essay: the DDA, the RTE, and the computation of scattering by plane parallel layers of particles. *J Quant Spectrosc Radiat Transf* 2017;189:43–59.
- [6] Ramezan pour B, Mackowski DW. Radiative transfer equation and direct simulation prediction of reflection and absorption by particle deposits. *J Quant Spectrosc Radiat Transf* 2017;189:361–8.
- [7] Mishchenko MI, Dlugach JM, Yurkin MA, Bi L, Cairns B, Liu L, et al. First-principles modeling of electromagnetic scattering by discrete and discretely heterogeneous random media. *Phys Rep* 2016;632:1–75.
- [8] Mishchenko MI, Dlugach JM, Liu L, Rosenbush VK, Kiselev NN, Shkuratov YG. Direct solutions of the Maxwell equations explain opposition phenomena observed for high-albedo solar system objects. *Astrophys J* 2009;705:L118–22.
- [9] Mishchenko MI, Dlugach JM, Mackowski DW. Coherent backscattering by polydisperse discrete random media: exact T -matrix results. *Opt Lett* 2011;36:4350–2.
- [10] Mishchenko MI, Liu L, Hovenier JW. Effects of absorption on multiple scattering by random particulate media: exact results. *Opt Express* 2007;15:13182–7.
- [11] Dlugach JM, Mishchenko MI, Liu L, Mackowski DW. Numerically exact computer simulations of light scattering by densely packed, random particulate media. *J Quant Spectrosc Radiat Transf* 2011;112:2068–78.
- [12] Väisänen T, Penttilä A, Markkanen J, Muinonen K. Validation of radiative transfer and coherent backscattering for discrete random media. In: *URSI international symposium on electromagnetic theory (EMTS)*; 2016. p. 396–9.
- [13] Mishchenko MI, Dlugach JM, Mackowski DW. Electromagnetic scattering by fully ordered and quasi-random rigid particulate samples. *J Opt Soc Am A* 2016;33:2144–9.
- [14] Mackowski DW, Mishchenko MI. Calculation of the T -matrix and the scattering matrix for ensembles of spheres. *J Opt Soc Am A* 1996;13:2266–78.
- [15] Mackowski DW, Mishchenko MI. A multiple sphere T -matrix Fortran code for use on parallel computer clusters. *J Quant Spectrosc Radiat Transf* 2011;112:2182–92.
- [16] Voit F, Schäfer J, Kienle A. Light scattering by multiple spheres: comparison between Maxwell theory and radiative-transfer-theory calculations. *Opt Lett* 2009;34:2593–5.
- [17] Penttilä A, Lumme K. Optimal cubature on the sphere and other orientation averaging schemes. *J Quant Spectrosc Radiat Transf* 2011;112:1741–6.
- [18] Mishchenko MI. *Electromagnetic scattering by particles and particle groups: an introduction*. Cambridge, UK: Cambridge University Press; 2014.
- [19] Mackowski DW, Mishchenko MI. Direct simulation of extinction in a slab of spherical particles. *J Quant Spectrosc Radiat Transf* 2013;123:103–12.

- [20] Lyot B. Recherches sur la polarisation de la lumière des planètes et de quelques substances terrestres. *Ann Obs Paris Sect Meudon* 1929;8:1–161.
- [21] Shkuratov Yu, Ovcharenko A, Zubko E, Miloslavskaya O, Muinonen K, Piironen J, et al. The opposition effect and negative polarization of structural analogs for planetary regoliths. *Icarus* 2002;159:396–416.
- [22] Rosenbush VK, Avramchuk VV, Rosenbush AE, Mishchenko MI. Polarization properties of the Galilean satellites of Jupiter: observations and preliminary analysis. *Astrophys J* 1997;487:402–14.
- [23] Rosenbush V, Kiselev N. Icy moons of the outer planets. In: Kolokolova L, Hough J, Levasseur-Regourd AC, editors. *Polarimetry of stars and planetary systems*. Cambridge, UK: Cambridge University Press; 2015. p. 340–59.
- [24] Dlugach JM, Mishchenko MI, Mackowski DW. Numerical simulations of single and multiple scattering by fractal ice clusters. *J Quant Spectrosc Radiat Transf* 2011;112:1864–70.
- [25] Van de Hulst HC. *Light scattering by small particles*. New York: Wiley; 1957.
- [26] Mishchenko MI, Yurkin MA. On the concept of random orientation in far-field electromagnetic scattering by nonspherical particles. *Opt Lett* 2017;42:494–7.
- [27] Mishchenko MI. On the nature of the polarization opposition effect exhibited by Saturn's rings. *Astrophys J* 1993;411:351–61.
- [28] Shkuratov YG, Muinonen K, Bowell E. A critical review of theoretical models of negatively polarized light scattered by atmosphereless solar system bodies. *Earth Moon Planets* 1994;65:201–46.
- [29] Tishkovets VP, Petrova EV, Mishchenko MI. Scattering of electromagnetic waves by ensembles of particles and discrete random media. *J Quant Spectrosc Radiat Transf* 2011;112:2095–127.
- [30] Muinonen K, Mishchenko MI, Dlugach JM, Zubko E, Penttilä A, Videen G. Coherent backscattering verified numerically for a finite volume of spherical particles. *Astrophys J* 2012;760:118.
- [31] Mishchenko MI, Dlugach JM. Can weak localization of photons explain the opposition effect of Saturn's rings. *Mon Not R Astron Soc* 1992;254:15P–18P.